Fields in the recycling cavity at LIGO Livingston Observatory

Andri M. Gretarsson*, Valery Frolov, Brian O'Reilly

LIGO Livingston Observatory, Livingston LA 70754, USA.

Erika D'Ambrosio†

LIGO Laboratory, California Institute of Technology,

MS 18-34, Pasadena, CA 91125, USA

Peter K. Fritschell

LIGO Project, Massachussetts Institute of Technology,

NW17-161, 175 Albany Street, Cambridge, MA 02139, USA

Abstract

We investigate the fields in a Pound-Drever-Hall locked, opically unstable, mode-mismatched Fabri-Perot cavity as a function of offset from resonance. The cavity under investigation was the recycling cavity of the Laser Interferometer Gravitational Wave Observatory (LIGO) detector in Livingston, Louisiana. In contrast to stable optical cavities, the shape of the resonating beam in the recycling cavity is very sensitive to microscopic cavity length changes around the resonance. This modifies the error signals used to control the recycling cavity length in such a way that the zero crossing no longer corresponds to the point of maximum power in the cavity nor to the point where the input beam mode is maximally resonant in the cavity. An FFT based optical model agrees well with the experimentally observed results. An analytical model, that takes into account the transverse distribution of the observed field in reflection from the cavity provides a qualitative demonstration of the mechanism by which the observed effects are generated. The effects described are important for the operation of power recycled gravitational wave interferometers.

* andri@ligo.caltech.edu

† ambrosio_e@ligo.caltech.edu

LIGO-T050040-00-D

I. INTRODUCTION

The LIGO [1–3] recycling cavity is designed to be optically stable at full input power, that means including the effect of thermally induced lensing as the recycling cavity optics heat up during full power operation [4, 5]. This article presents measurements of the fields in the recycling cavity when the input power is set low enough that no significant thermal lensing occurs. In this state the recycling cavity is optically unstable in the sense that it is not mode selective and therefore the recycling cavity beam is not matched to the optical mode of interferometer arms. In fact, the fields in the cavity and on reflection exhibit rings generated by the interference of the cavity field with the input beam, and even small angle or length perturbations of the cavity have a significant effect on the features of the circulating field. As a result, the Pound-Drever-Hall error signal [6] used to control the length of the cavity is no longer zero at the point of maximum cavity power.

We investigated this issue by applying a series of offsets to the error point of the length loop while recording the power in the cavity and acquiring images of the light distribution in the cavity and on reflection. The results were then compared to a paraxial, FFT-based numerical model [7]. Although the numerical model has previously been used to simulate aspects of the LIGO Livingston interferometer [8], this is first time simulation results from the model have been compared with measured data from the interferometer. We interpret the results of the measurements and of the numerical model with the help of a simple analytical description which, despite its simplicity, demonstrates the important features we are interested in.

II. MEASUREMENT OVERVIEW

The field circulating in the recycling cavity and the field reflected from it are investigated as functions of small length offsets with respect to what is the resonant length, according to the Pound-Drever-Hall servo technique. Field data have been recorded for several different length offsets around the length set by the cavity locking servo. In order to vary the cavity length, we changed the error point of the servo while locked on a resonance. In this way we could change the length of the recycling cavity by several nanometers before lock was lost. To make the interpretation of the optical fields simpler, most of our measurements

were taken when the arms were not locked but the recycling cavity was locked on the carrier and the sidebands are almost fully reflected from the cavity. In this state, the carrier can be expected to behave similarly to the sidebands in the full interferometer lock. As a qualitative check, we also made measurements with the full interferometer locked. In the fully locked state, the sidebands are resonant in the recycling cavity but antiresonant in the arm cavities while the carrier field is resonant in all cavities.

To obtain information about the intensity distribution we used two CCD cameras (one capturing the light reflected from the cavity and the other capturing the light picked out of the cavity by means of the slightly wedged antireflective side of one of the mirrors). To measure the power in the cavity we used a calibrated photodiode operating at DC measuring the intensity of the beam picked off of the slightly wedged antireflective side of the beamsplitter. (The beam picked off from the antireflective side of the beamsplitter, like the beam picked off from the antireflective side of the arm input test masses, is a good representation of the recycling cavity beam.)

In all cases care was taken that the beams do not overfill the photodiode apertures. In the case of the fully locked interferometer, we used different methods to provide information about the sidebands in the recycling cavity. Since the field intensity is dominated by the carrier we could not use a photodiode or a CCD camera for our purpose of interrogating the RF sidebands. To measure the intensity of the sidebands, we used an RF photodiode whose signal is demodulated at twice the sideband frequency. This photodiode received a highly focused version of the beam picked off from the antireflective side of the beamsplitter. Once again, care was taken that the beam did not overfill the photodiode aperture. The signal from this photodiode is proportional to the geometric mean of intensity of the upper and lower sidebands. We employed a similar technique to measure the spatial profile of the sideband intensity with the phase camera [9]. By rapidly scanning an enlarged version of the beam from the recycling cavity over an RF photodiode, which is now greatly overfilled, we could reconstruct the spatial profile of the geometric mean of the sideband intensity. The phase camera received the recycling cavity beam picked off from the slightly wedged antireflective side of ITMY (the input mirror for one of the arms).

III. FFT MODEL OVERVIEW

We refer to the numerical model with which we compare our measurements as 'The FFT Model'. The FFT Model is a numerical tool for beam propagation implemented by Fast Fourier Transform [7]. Propagation is calculated using the paraxial approximation and the field is transformed to the frequency domain before multiplication with the (Fourier transform of the) propagator. At each optic, the field is transformed back to the space domain and its interaction with the optic is evaluated on a 128x128 grid. In our case, each pixel of the field was simply multiplied by a phase delay according to the profile of the mirror. To calculate the fields in a resonant cavity such as the LIGO Livingston recycling cavity, the propagation was iterated until the resulting field grid became stationary. Once the fields had been modeled, they were used to construct (post-hoc) the Pound-Drever-Hall error signal generated by the cavity. In this way we could compare the measured error signal with the simulation. This process was repeated for several microscopically different cavity lengths to get the error signal and field distributions as a function of cavity length.

IV. CARRIER LOCK IN THE RECYCLING CAVITY

Figure 1 compares the resonant field intensity derived from the FFT model with the actual measured field intensity as a function of cavity length. (Measurement and calculation refer to light picked off from the low-reflective side of ITMY). The light distribution is dramatically different for even small changes in the cavity length. The main theme of this paper is to relate this effect to small changes in the error signal. Note that the FFT model faithfully reproduces the measured beam shape as it goes from a one-peak profile to a donut and also shows the correct relative increase in beam size.

Figure 2 compares the measured cavity power with the prediction from the FFT model. Given that there are no free parameters, the agreement is reasonably good. In particular, the point of maximum power found by the FFT model agrees with the measurement. The fact that the measured cavity power values fall slightly below the prediction for the largest length offsets is probably due to loop gain reduction which produces a change in the calibration of the length offset. This causes an underestimation of the cavity length variation for offsets far from the point of maximum cavity power. The figure also shows the power in the TEM_{00}

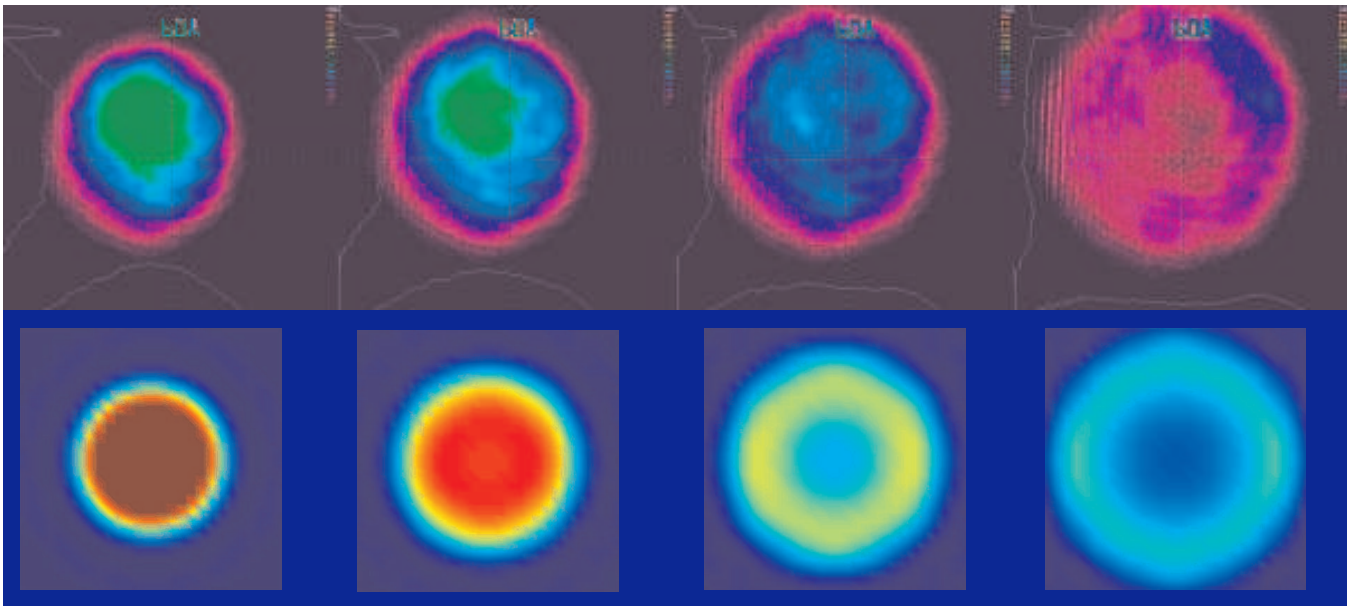

FIG. 1: Effect of changing the cavity length by several nanometers on the shape of the carrier resonating in the recycling cavity. (Arms are not resonant.) Comparison of actual image captures with model predictions. The top row shows a false color image of the intensity of the recycling cavity beam picked off at ITMY. The colors represent intensity. The bottom row shows the FFT model results and correspond to the same length offsets, applied to the value established by the servo. From left to right and for both simulation results and experimental observations, the offsets are: **-8nm**, **-4nm**, **0nm**, and **+4nm**. For reference, the diameter of the ring structure in the rightmost image in the bottom row is 5 cm. Since we do not know the absolute scale of the captured images in the top row we matched the overall scale of the captured images to that of the model images by eye. But there was no relative scaling of images within each set.

part of the cavity field, that is the mode of the beam incident on the recycling mirror (fundamental optical mode of the modecleaner propagated through the input telescope). The FFT model shows that the TEM_{00} component is maximized even further from the locking point than the total cavity power. This means that the Pound-Drever-Hall locking scheme chooses a cavity length which corresponding neither to the maximum total power nor to the maximum TEM_{00} power.

To gain insight into this unexpected behavior, we used an analytical expression for the Pound-Drever-Hall error signal on reflection, that was motivated by our observations of the actual reflected field distribution. We first describe a general formula for the Pound-Drever-

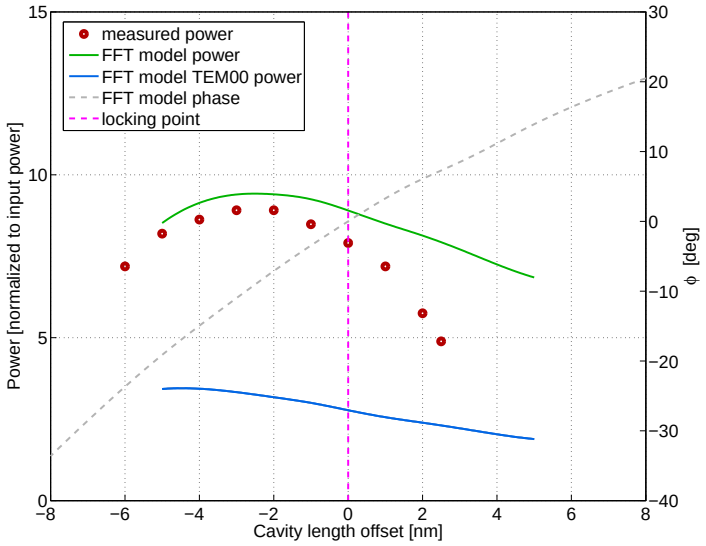

FIG. 2: Power in the recycling cavity as a function of cavity length offset. FFT Model accurately predicts the length offset at which the cavity power is maximized. The green line shows the FFT model prediction for the total cavity power shown. The blue line shows the FFT model prediction for the power in the TEM00 component.

Hall error signal that does not make any assumption about the spatial profile of the beams. Our notation is defined in Fig. 3 which shows a schematic of the recycling cavity.

The Pound-Drever-Hall error signal is generated by phase modulating the input beam, before the cavity

$$\begin{aligned} \Psi_{IN} &= \Psi_{\rm LASER} \exp[i\Gamma \cos\omega t] \\ &\simeq J_0(\Gamma)\,\Psi_{\rm LASER} + iJ_1(\Gamma)\,\Psi_{\rm LASER} \exp[i\omega t] + iJ_1(\Gamma)\,\Psi_{\rm LASER} \exp[-i\omega t] \\ &\equiv \Psi_{IN}^{CR} + \Psi_{\rm IN}^{SB+} \exp[i\omega t] + \Psi_{\rm IN}^{SB-} \exp[-i\omega t] \end{aligned} \tag{1}$$

where ω is the modulation frequency and Γ is the modulation depth. The input field can therefore be considered as three collinear beams: the carrier, Ψ_{IN}^{CR}, and a pair of sidebands, $\Psi_{\rm IN}^{SB+}$ and $\Psi_{\rm IN}^{SB-}$, with frequency separation ω on either side of the central frequency of the carrier. The 24.5 MHz modulation frequency is such that when the carrier beam is on resonance in the recycling cavity, the sidebands are nearly on anti-resonance, and their

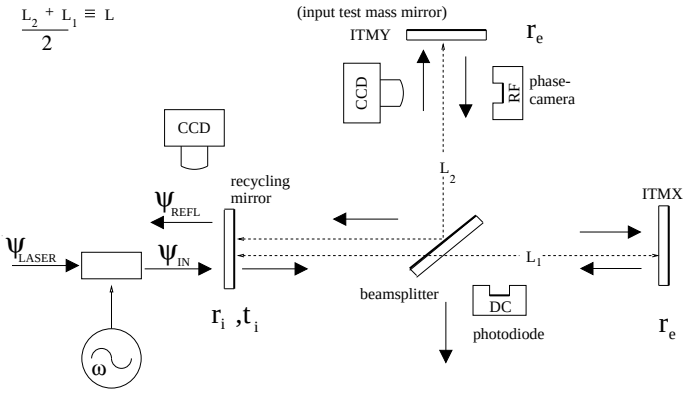

FIG. 3: The laser field $\Psi_{\rm LASER}$ is phase modulated to produce $\Psi_{\rm IN}$ consisting of approximately 90% carrier light and 5% each upper and lower phase modulation sidebands, 25 MHz on each side of the carrier. The reflected field $\Psi_{\rm REFL}$ is the sum of three components. The contributions are given by: the sidebands which are almost completely reflected back towards the laser due to the cavity length being set so they are not resonant, the prompt reflection of the carrier that is not interacting with the recycling cavity, and the leakage of that portion of carrier field that is resonating inside the cavity. The latter component of the total beam is split by the beam splitter into two paths of slightly different lengths, represented in the diagram by the overall phases φ_i. The amplitude transmission and reflection coefficients are represented by t_i and r_i respectively. The position of the beam splitter is actively controlled, so that its antisymmetric port corresponds to the dark fringe of the carrier.

interaction with the cavity is minimal. Therefore, of the three input fields, only the carrier is sensitive to the geometrical features of the cavity (such as length or alignment):

$$\begin{aligned} \Psi^{SB-}_{\rm REFL} &\simeq -\Psi^{SB-}_{\rm IN} \\ \Psi^{SB+}_{\rm REFL} &\simeq -\Psi^{SB+}_{\rm IN} \\ \Psi^{CR}_{REFL} &= D\Psi^{CR}_{IN} \end{aligned} \tag{2}$$

where D describes the effect of the cavity on the resonating beam. The total reflected power

is the integral of the squared field, corresponding to the sum of the three fields

$$\begin{aligned} P_{\rm REFL} \;=\; & \int_S |\Psi_{\rm REFL}|^2\, dS = \int_S \{ |\Psi^{CR}_{\rm REFL}|^2 + |\Psi^{SB+}_{\rm REFL}|^2 + |\Psi^{SB-}_{\rm REFL}|^2 \\ & + 2\Re\left[(\Psi^{CR}_{\rm REFL} {\Psi^{SB-}_{\rm REFL}}^* + \Psi^{SB+}_{\rm REFL} {\Psi^{CR}_{\rm REFL}}^*) \exp(i\omega t) \right] \\ & + 2\Re\left[\Psi^{SB+}_{\rm REFL} {\Psi^{SB-}_{\rm REFL}}^* \exp(2i\omega t) \right] + \ldots \} \, dS \end{aligned} \tag{3}$$

where S indicates an area of integration much larger than the beam. To lock the cavity, we need to control both the common mode length of the cavity (sum of the two x and y paths of the cavity) and the differential mode length (difference of the x and y pathlengths). As mentioned in Section II, this is done using the Pound-Drever-Hall technique. The differential mode length is controlled using the very small amount of sideband light, transmitted through the recycling mirror and detected at the antisymmetric port. In this paper we are concerned with the role of the common length of the cavity. This corresponds to a sort of cavity average length and is controlled by the same techniques used for any cavity length, that is using $P_{\rm REFL}$. The error signal, V_I, is the I-phase of the demodulated voltage from a photodiode placed at the reflected port. The demodulation frequency is the same as the phase modulation frequency ω, so one term survives

$$\begin{aligned} V_I \;\approx\; & \alpha \int_S dS \int_0^T dt \, \frac{P_{\rm REFL} \cos(\omega t)}{T} \\ =\; & \alpha \int_S \Re(\Psi^{CR}_{\rm REFL} {\Psi^{SB-}_{\rm REFL}}^* + \Psi^{SB+}_{\rm REFL} {\Psi^{CR}_{\rm REFL}}^*) \, dS \end{aligned} \tag{4}$$

where $T \gg \omega^{-1}$ is the time constant of the demodulation and α is an overall (real) constant. This can be written more simply as

$$\begin{aligned} V_I \;\propto\; & \Re\left[\langle \Psi^{CR}_{\rm REFL} | \Psi^{SB-}_{\rm REFL} \rangle + \langle \Psi^{SB+}_{\rm REFL} | \Psi^{CR}_{\rm REFL} \rangle \right] \\ =\; & 2 J_1(\Gamma) \, \Im \langle \Psi_{\rm LASER} | \Psi^{CR}_{REFL} \rangle \, . \end{aligned} \tag{5}$$

If the input beam is modematched to the cavity and the cavity is optically stable, then the reflected carrier will have the same shape as the input beam and the amplitude and phase

are modified by the cavity in the standard way.

$$\begin{aligned} \Psi_{\text{LASER}} &= \sqrt{\tfrac{2}{\pi w^2}} \exp\left(-r^2/w^2 + i\tfrac{\pi r^2}{\lambda R}\right) \\ \Psi^{CR}_{\text{REFL}} &= t_i^2 r_e\, e^{i\phi}/(1 - r_i r_e\, e^{i\phi})\ \Psi_{\text{LASER}} \end{aligned} \tag{6}$$

where r is the radial distance from the beam axis, λ is the wavelength, w is the width of the input beam and R is the radius of curvature of the input beam, t_i, r_i, and r_e are the mirror amplitude transmission and reflection coefficients (see Fig. 3). The angle ϕ is the returning carrier phase, defined by $\phi \equiv 4\pi\delta L/\lambda$, where δL is the cavity length change about resonance. The error signal from Eq. (5) is then

$$V_I \propto \Im\left\{\frac{r_i r_e t_i^2}{(r_i r_e - e^{i\phi})}\right\}. \tag{7}$$

and taking the imaginary part

$$V_I \propto \frac{2 r_i r_e t_i^2}{(1 + r_i^2 r_e^2 - 2 r_i r_e \cos\phi)}\ \sin\phi. \tag{8}$$

For small ϕ we get the well known result that the error signal from a mode-matched cavity is proportional to the returning carrier phase and thereby proportional to the cavity length near resonance.

Equation (5) makes it obvious that the error signal is generated only from the component of the reflected carrier that is in the mode of the laser. Therefore, for stable cavities, Pound-Drever-Hall technique maximizes the power in the mode of the input beam (TEM_{00} in our basis). However, if the transverse shape of the reflected carrier also depends on the cavity length, as may occur in unstable cavities, the Pound-Drever-Hall technique need not maximize the power in the TEM_{00} mode component. In addition to the usual length effect, the amplitude and phase of the TEM_{00} component of the reflected carrier now vary due to the changing the spatial profile. Thus, the error signal in Eq. (5), and consequently the lock point chosen by the servo, involves a competition between the length and spatial changes. This induces a length offset with respect to the lock point of a stable cavity. Our mode-mismatched marginally unstable recycling cavity appears to exhibit this effect. A photograph of the beam at the reflected port which is dominated by carrier light shows clearly that the reflected carrier is not in the TEM_{00} mode of the input beam (Fig. 4) and

the shape of the cavity beam changes as a function of length (Fig. 1). A similar change is seen in the reflected carrier.

To demonstrate the mechanism by which a length offset is generated, we now choose an analytic representation of the reflected carrier field (intensity shown in Fig. 4). We then use this analytic representation of the field to calculate the Pound-Drever-Hall error signal as a function of cavity length. We assume that the reflected carrier has the functional form of Newton's Rings [10]. In reality of course, the field is generated by a superposition of many cavity phasefronts interfering with the promptly reflected beam and is not simply the classical superposition of two beams with different phasefront curvatures. Nonetheless, this model is sufficient to demonstrate the important effects. We take

$$\Psi^{CR}_{\rm REFL} = r_i \Psi_{\rm LASER} - \frac{t_i^2 r_e\, e^{i\phi}}{1 - r_i r_e\, e^{i\phi}} \sqrt{\frac{2}{\pi w^2}} \exp\left(-r^2/w^2 + i\frac{\pi r^2}{\lambda R'}\right) \tag{9}$$

where R' is the radius of curvature of the leakage beam from the cavity. The optical phase ϕ is the returning carrier phase. In this simple model, ϕ is also the phase of the field at the center of the reflected port beam with respect to a dark center. Therefore, it is in prinicple possible to obtain ϕ from a fit of the intensity. Unfortunately, the intensity image of Fig. 4 is saturated in the center. The camera has limited dynamic range, and in order to see the faint outer fringes we set the light level so that the central few fringes were saturated. However, it is also be possible to obtain the phase angle ϕ by fitting the radial width of the bright rings, normalized to the radius of the first bright ring. It's not difficult to show that Eq. (9) leads to the following expression for the radii r_n of the bright fringes, normalized to the radius of the first fringe

$$r_n = \sqrt{\frac{2n\pi - \theta}{2\pi - \theta}}, \qquad n = 1, 2, 3, \ldots \tag{10}$$

where

$$\theta = \mathrm{Arg}\left(\frac{t_i^2 r_e e^{i\phi}/r_i}{1 - r_i r_e e^{i\phi}}\right) \tag{11}$$

Figure 5 shows a fit of Eq. (10) to the measured reflected port bright fringe positions, giving $\theta = 229.4° \pm 3°$[11]. The goodness of the fit in Fig. 5 suggests that the spatial form of the carrier at the reflected port is indeed not very different from that of Newton's Rings. However, the range of Eq. (11) for $\phi \in [0°, 360°\rangle$ is only $[-90°, 90°\rangle$ which does not accommodate the value of θ found from the fit. This is a reflection of the fact that our model is an oversimplification of the actual mechanism by which the field is generated. Yet,

FIG. 4: The effect of mode mismatch into the cold recycling cavity. Image taken from a CCD camera at the reflected port.

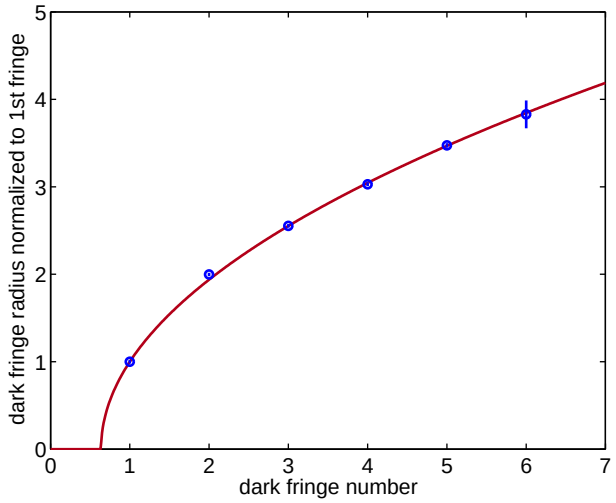

FIG. 5: Radius of dark regions of circular fringes at the reflected port with zero applied PRC offset. The data has the form expected from Newton's rings.

as we see below, the qualitative behavior of the model mimics what is observed. When we calculate the error signals due to the Newton-Ring-like structure of the reflected beam

inserting Eq. (9) into Eq. (5) and performing the overlap integral, we get

$$V_I \propto -\Im\left\{\frac{r_i r_e t_i^2}{(r_i r_e - e^{i\phi})(1-\rho)}\right\}. \tag{12}$$

where

$$\rho \equiv \frac{i\pi w^2}{2\lambda}\frac{(R'-R)}{RR'} \tag{13}$$

The limit of Eq. (12) when $R' \to R$ is identical with Eq. (7). Taking the imaginary part, we obtain

$$V_I \propto \frac{r_i r_e t_i^2}{(1 + r_i^2 r_e^2 - 2 r_i r_e \cos\phi)(1+\rho^2)}\left[\sin\phi - (r_i r_e - \cos\phi)\rho\right]. \tag{14}$$

When $\phi \to 0$, the first term disappears but the term proportional to ρ remains. This is the source of the loop offset. The terms of this equation represent the competition between the usual error signal and the length dependent contribution of the TEM_{00} mode to the spatial structure of the cavity field.

A plot of the error signal from Eq. (12) as a function of δL, using R, w, r_i, r_e and λ for the Livingston interferometer, is shown by the red trace in Fig. 6. The loop offset is obvious.The grey trace is the error signal for a mode matched, stable cavity from Eq. (7), using the same parameters. Infact the loop offset is quite robust under large changes in R' and it varies from roughly 1 nm for $R' = 2R$ to 5 nm as R' progresses through being flat to $R' = -R$ (the case shown). This plot also suggests an explanation for why we found it possible to put a four or five times larger loop offset in one direction than the other. The turn-over point of the error signal is much more quickly reached by offsets in one direction than the other.

The agreement between the experimental observations and the FFT optical model indicates that the measured loop offset is an optical effect and is not due to electronics offsets or other imperfections of the apparatus. The transverse field structure changes as a function of the microscopic length change and this is a general property of marginally unstable cavities, as demonstrated by our analytic model that holds for any similar situation and explains the fundamental mechanisms beneath the observed loop offset. The resonant points of such cavities locked with the Pound-Drever-Hall method may need to be adjusted by hand to compensate for the optically generated loop offset.

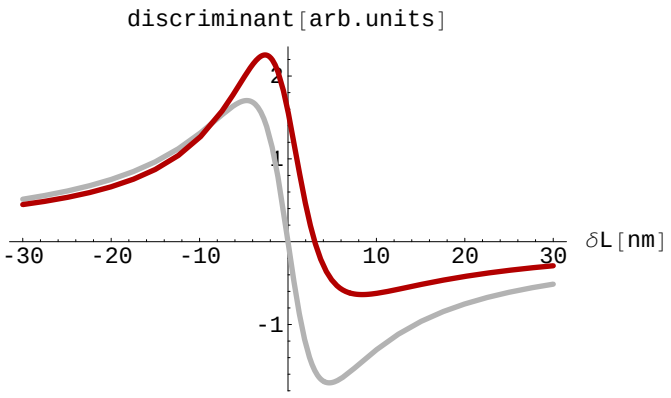

FIG. 6: The error signal as a function of δL calculated assuming a Newton-Ring-like structure for field reflected from the cavity, red curve, compared with the ideal error signal, blue curve.

V. FULL INTERFEROMETER LOCK

When the full interferometer is locked, the intensity in the recycling cavity is dominated by the carrier, whose spatial structure is set by the arm to be the TEM_{00} mode of the arm. The arms are optically stable and they only resonate on a single cavity mode. When the full interferometer is locked, the arm cavity mode is the only one with the necessary frequency and transverse shape, allowing it to resonate in both the recycling cavity and the arms. The sidebands on the other hand, being non-resonant in the arms, experience almost the same conditions as they do when the recycling cavity is locked without the arms. Therefore, we can expect that the field structure of the sidebands in the full lock should be qualitatively similar to the carrier field distribution of Section IV. Since the intensity of the carrier in the recycling cavity is much larger than that of the sideband during a full lock, we could not use a CCD camera to investigate the sideband beam profile. To extract an image of the sideband profile in the cavity, we used the phasecamera. Images of the sideband intensity taken from the beam picked off of the antirefltective side of ITMY are shown in Figure 7. The colors in this image stand for the geometric mean of the intensity of the two sidebands. For technical reasons, we did not obtain a calibration of the offset in terms of length.

Figure 8 shows the sideband intensity normalized to the total side band intensity in the input beam (monitored at the LIGO Livingston observatory by the NSPOB channel) as the cavity length is changed (the PRC_offset trace). The x-axis shows the offset added

to the error point in uncalibrated counts. Note that we see a much larger change in the sideband intensity in this fully locked state than the change in the carrier intensity for the carrier lock in the recycling cavity. The reason for this is most probably that as the profile of the sidebands in the recycling cavity begins to better match the resonating mode of the arm cavities, a larger fraction of the beam is exactly on antiresonance and is totally reflected. Despite the fact the entire situation is different for a full interferometer lock, as the arms have a very high Finesse and are very selective in terms of cavity modes, we see that the qualitative features are the same as those of Section IV. The shape of the cavity beam changes as a function of length and the lock point does not correspond to maximum sideband power in the cavity. Although we could not extract the TEM_{00} component of the sidebands, we can assume that it is also not maximized.

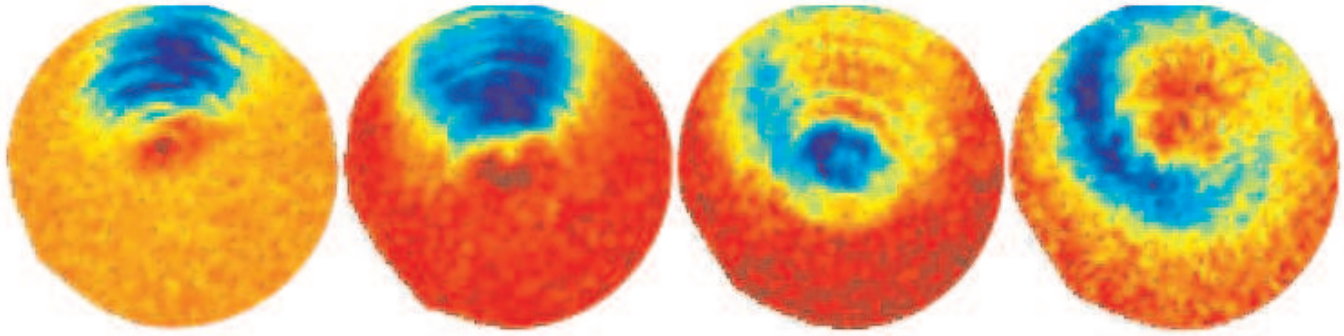

FIG. 7: Effect of changing the cavity length by several nanometers on the shape of the sidebands resonating in the recycling cavity. The colours represent the geometric mean of the intensity of the upper and lower sidebands.

Acknowledgements

The measurements described were performed on the LIGO interferometer at Livingston (Lousiana) whose continuing operation is made possible by the hard work of many people. The authors are indebted to these people and to the LIGO collaboration for the use of the instrument. Rana Adhikari and David Ottaway gave us insightful comments during our initial observations. Support for LIGO research projects comes from the National Science

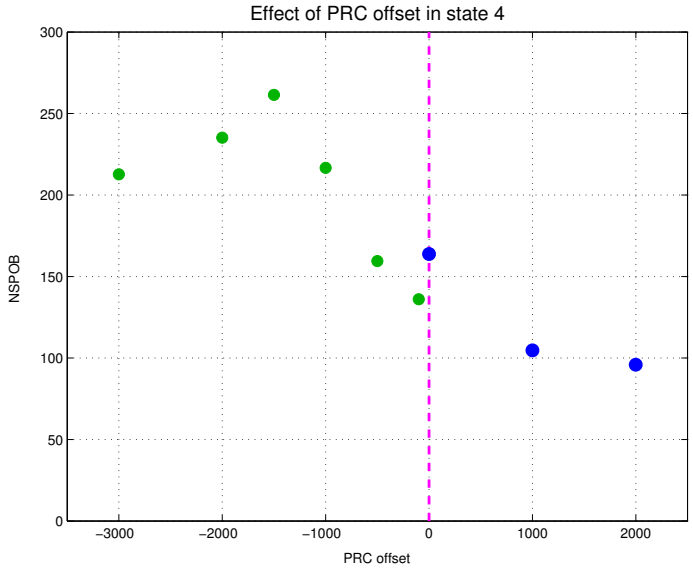

FIG. 8: Sideband intensity as a function of uncalibrated length offset. This graph contains data from two lock stretches which we have distinguished by the green and blue colours.

Foundation (USA) grant number PHY-9210038.

---

[1] Abbott et al., Nucl. Instr. and Methods **A517**, 154 (2004).

[2] A. Abramovici et al., Science **256**, 325 (1992).

[3] P. Fritschel, Applied Optics **40**, 4988 (2001), http://adsabs.harvard.edu/abs/2001ApOpt..40.4988F.

[4] R. Beusoleil, E. D'Ambrosio, B. Kells, J. Camp, E. Gustafson, and M. Fejer, J. Opt. Soc. Am. B **20**, 1247 (2003).

[5] B. Kells and J. Camp, http://www.ligo.caltech.edu/docs/T/T970097-01.pdf (1997).

[6] R. W. P. Drever et al., Applied Physics B **31**, 97 (1983), description of the Pound-Drever-Hall method.

[7] B. Bochner, http://www.ligo.caltech.edu/docs/P/P980004 (1998), fFT Model Description.

[8] E. D'Ambrosio, Class. and Quant. Gravity **21**, 1113 (2004).

[9] K. Goda, D. Ottaway, B. Connelly, R. Adhikari, N. Mavalvala, and A. Gretarsson, Opt Lett **29**, 1452 (2004), URL `http://eutils.ncbi.nlm.nih.gov/entrez/eutils/elink.fcgi?cmd=p%rlinks\&dbfrom=pubmed\&retmode=ref\&id=15259710`.

[10] F. A. Jenkins and H. E. White, *Fundamentals of Optics, 4th Ed* (McGraw-Hill, 1976).

[11] If the sign of the radius of curvature of the cavity beam is taken to be opposite to that of the input beam, a slightly different equation for the fringe distance arises with $n = 0, -1, -2, -3, \ldots$. Fitting for that case we obtain $\theta = 130.6^\circ \pm 3^\circ$. This possibility does not affect the conclusions.